DESIGN OF JOINTS OF COMPOSITE MEMBERS WITH CURVILINEAR REINFORCEMENT STRUCTURE

A. Malakhov[*], A. Polilov

Institute of Machines Science named after A.A. Blagonravov of the Russian Academy of Sciences, Department of Strength, Survivability and Safety of Machines, Malyy Kharitonyevskiy pereulok 4, Moscow, Russia
*e-mail address of the corresponding author (anmaviko@gmail.com)

Abstract
This paper describes a junction between a composite plate and a metal component as well as a method of modelling a heterogeneous composite structure with curvilinear reinforcement. In the present case, fastening between the metal component and the composite plate is realized by means of a steel bolt. Curvilinear trajectories of fibres are modeled for the plate. They are adapted to the geometry of the plate and current loading. The functionally graded material is simulated on the basis of these trajectories. Fibre orientation and fibre volume fraction are heterogeneous throughout the plate. It appeared that load-carrying capability of the created structure with the curvilinear reinforcement increases by 8.2 times in comparison with the structure having the rectilinear reinforcement.

1. Introduction

The disadvantage of composite structures is their weak fastening joints as a result of the traditional perforation technology for rivets or bolts. Nature suggests an alternative approach to the design of composite structures: producing joints without cutting fibres and using a curvilinear reinforcement structure such as in the 'branch-trunk' or 'trunk-root' junctions of wood.

Different methods have been developed to reduce stress concentrations for composite structures. Many early works for reducing of the stress concentrations describe the shape optimization [1-5]. Various reinforcements can be used to reduce the stress concentrations as in [6]. Many methods apply the possibilities of varying the stiffness into composite structures [7-12]. The modelling methods of curvilinear reinforcement structures use changing the fibre orientation. The fibre orientations were arranged along the maximum principal stress in each element for a composite plate with a hole to simulate the structure [7,8]. The value of the stress concentration factor along fibres reduces from 7 to 4 for the structure [7] but shear stress is practically equal to zero [8]. There is another approach where the fibres orientations were optimized in a composite plate having a hole [9]. It appeared that the value of the stress concentration factor along fibres for the structure reduces from 7 to 1.5. All these methods

demonstrate that the stress concentrations can be reduced by the curvilinear reinforcement structures and consequently lead to increasing of load-carrying capability.

The paper describes the design of joints between composite and metal components as well as a modelling method for composite structures with curvilinear reinforcement that allows the trajectories of fibres to be adapted to geometric discontinuities (holes, notches, bolts and so on). The main idea of such joints is that an embedded metal ring is inserted into a composite part and metal members are joined to this ring in the usual way. The ring is a geometric discontinuity in the composite part. The trajectories of fibres are adapted to the geometric discontinuity and current loading before the curvilinear reinforcement structure is simulated. In this case, the connection of the embedded ring and a metal member with a metal bolt is considered.

2. Definition of the problem

This investigation focuses on modelling a heterogeneous composite plate. Fibre orientation and volume fraction of fibres change locally through the plate from point to point. An embedded ring is inserted into the composite plate. To join the ring and a metal member a steel bolt is used. The dimensions of the rectangular plate are shown in Figure 1 where its length = 135 mm and its height = 80 mm. The outer radius of the embedded ring is $R_1 = 10$ mm; the inner one is $R_2 = 8$ mm. The radius of the bolt is 8 mm. Because of the symmetrical geometry, material and boundary conditions only half of the plate is analysed.
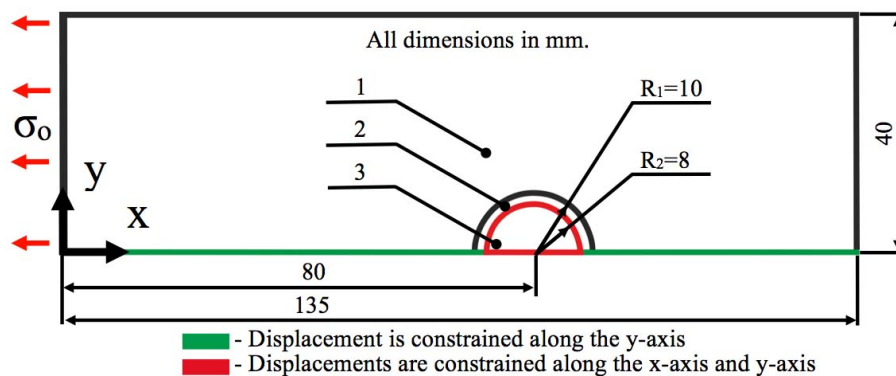

Figure 1. Dimensions and boundary conditions; 1– composite plate, 2 – ring, 3 – bolt.

Stress of $\sigma_o = 1$ Pa is applied to the left side of the plate. The bottom part of the plate and the embedded ring have a constrained degree of freedom in vertical displacement along the y-axis when y = 0 mm. An outer profile of the bolt is constrained in vertical and horizontal displacements along the x-axis and y-axis. A contact surface is simulated between the composite plate and the ring. A contact surface between the ring and the bolt is simulated in the same way. The friction coefficient for the contact surfaces is zero. The boundary conditions are shown in Figure1.

The solution of the problem is obtained by means of the finite element method (FEM) using ANSYS software. Two-dimensional quadrilateral elements are used in the calculation model. The ring and the bolt are modelled from isotropic material. Properties of the steel A36 [13] for the bolt and the embedded ring are: E = 200 (GPa) и μ = 0.26. Each element of the heterogeneous composite plate has its own orthotropic material. The elastic material constants

of the orthotropic material depend on the fibre volume fraction, which is not homogeneous along the coordinates of the plate. More detailed information about the modelling of composite material is given in section 3.

3. Modelling method for functionally graded material

3.1. General scheme

After simulation of the geometry of the structure, material and boundary conditions, the stress fields are obtained. The solution is obtained with the FEM. It should be noted that an orthotropic material for the whole plate is used for the first iteration. As a result the distribution of fibre trajectories is received with no shear stress along these fibre trajectories. On the basis of these trajectories, the functionally graded material (FGM) is simulated. Each element of this structure has its own mechanical properties depending on the distribution of fibres. The fibre direction is modelled by assigning to each element its own local coordinate system, which is arranged along the maximum principal stress that corresponds to the fibre direction. A change of the volume fraction of fibres depends on the distribution of the fibres obtained. The elastic material constants change according to the fibre volume fraction. Fibre orientation and material properties are constant within an element. Thus, the created discrete model takes into account the local change of direction and the volume fraction of fibres. After local material properties are assigned to each element, the stress state in the new structure changes. The new structure has other trajectories of fibres conforming to the new stress state. The solution of this problem has an iterative character and the process will end when the field of stresses from iteration to iteration is not practically changed.

3.2. Modelling of curvilinear fibre trajectories

The solution for creating fibre trajectories is achieved by a numerical method. The strain-stress state is calculated by the FEM. The general algorithm scheme looks as follows. Knowing the field of stresses in elements, it is possible to find the angle β for any point of the structure along which shear stresses are zero. Varying the length of the segment Δ, which depends on the stress gradient, and defining the angle β, one can build a row of sequential points. From this row a trajectory of principal stresses can be created along which shear stresses are zero. Thus, the required curvilinear trajectories of the principal stresses are obtained. With these trajectories FGM can be simulated. The method for creating fibre trajectories is described in more detail in [14].

3.3. Simulation of fibre orientation and mechanical structure properties

3.3.1. Simulation of fibre orientation

After the curvilinear trajectories of fibres are determined, fibre orientations and mechanical structure properties are simulated. To simulate fibre orientation a local coordinate system is used. A local coordinate system is assigned to each element of the heterogeneous composite plate. The origin of coordinates is located in the centre of an element and its x-axis is directed along the maximum principal stress.

3.3.2. Simulation of mechanical structure properties

Each element of the structure corresponds to its local volume fraction of fibres, which depends on the obtained distribution of fibre trajectories. In this case, the volume fraction of fibres depends on the distance between the fibres. For each ith element located inside the first zone the distance between the fibres is calculated in the following way. Two normal lines are drawn from the centre of the ith element to the nearest fibre trajectories. The sum of two lengths of created segments (a_i, b_i) gives the required distance between the fibres for ith element (Figure 2). After the distance is obtained for each element from the first zone, the volume fraction of fibres is calculated. Let us suppose that the maximum volume fraction of fibres ($V_{fmax} = 0.577$) [15] is assigned to the kth element, which has the smallest distance ($a_k+b_k = \min(a_i+b_i)$). Then with Equation (1) the volume fraction of fibres V_{fi} for all ith elements is obtained:

$$V_{fi} = V_{fmax} \times (a_k + b_k) / (a_i + b_i) \tag{1}$$

A specific orthotropic material is assigned to each element of the structure. Its elastic material constants depend on the volume fraction of fibres. Elastic moduli and Poisson's ratio are calculated by Equations (2) taken from [16]:

$$\begin{aligned}
E_1 &= V_f \times E_{1f} + (1 - V_f) \times E_{1m} \\
E_2 &= E_{2f} \times E_{2m} / (V_f \times E_{2m} + (1 - V_f) \times E_{2f}) \\
G_{12} &= G_{12f} \times G_{12m} / (V_f \times G_{12m} + (1 - V_f) \times G_{12f}) \\
\mu_{12} &= V_f \times \mu_{12f} + (1 - V_f) \times \mu_{12m},
\end{aligned} \tag{2}$$

where E_{1f}, E_{2f}, G_{12f} are Young's moduli for fibre, E_{1m}, E_{2m}, G_{12m} are Young's moduli for matrix and μ_{12f}, μ_{12m} are Poisson's ratios for fibre and matrix respectively.
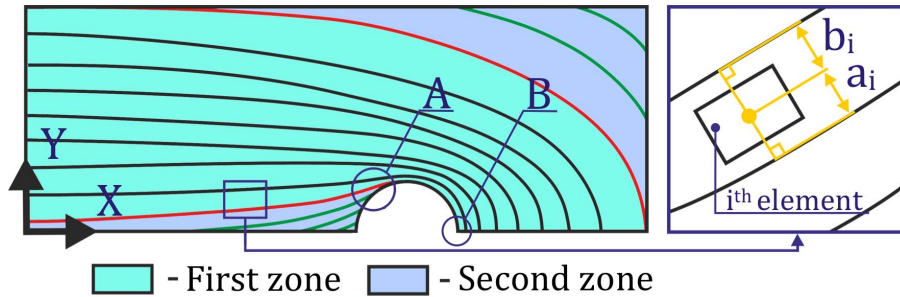

Figure 2. The first zone and the second zone for the plate.

The mechanical properties for the carbon fibre and the matrix used in the analysis are given in Table 1 [17]. Knowing the volume fraction of fibres in each element and the elastic material constants for the fibre and the matrix, the mechanical properties of orthotropic material are calculated using Equations (2). Therefore the number of these orthotropic materials is equal to the number of elements of composite plate.

	E$_1$ (GPa)	E$_2$ (GPa)	G$_{12}$ (GPa)	μ_{12}
Fibre	276	19.5	70	0.28
Matrix	4.76	4.76	1.74	0.37

Table 1. The mechanical properties for carbon fibre and matrix.

3.3.3. FGM modelling features

Unfortunately, the above-described modelling method cannot be used for the second zone (Figure 2) because it is impossible to calculate the distance between fibres. That means another approach needs to be applied to the zone. For the second zone four FGM modelling methods were developed. The first three methods have both strong and weak points. They cannot solve the two following problems simultaneously, however:

(1) provide the iterative process;
(2) eliminate singular elements in zone A (Figure 2), which are located in the area between the opening and the bottom fibre.

The fourth method solves both problems, which is why it was used in the current analysis. The main purpose of the method is to assign the fibre orientations and the volume fraction of fibres of the top and bottom trajectories (marked in red in Figure 2) to the elements located inside the second zone. Let us consider this algorithm in more detail. First, depending on the x coordinates the values of fibre orientations (β) and the volume fraction of fibres (V_f) are gathered along the top and bottom trajectories. Thus, the functions $\beta(x)$ and $V_f(x)$ are formed. Second, depending on x the values (β and V_f) are set for elements from the second zone. It appears that the fibre orientations and the fibre volume fraction for the second zone with respect to the coordinate y are the same, i.e. the simulated trajectories of fibres for the second zone (marked in green in Figure 2) are parallel to the top and bottom trajectories. Thus, the FGM is simulated for the second zone.

4. Results and discussion

After the iterative process was completed, the next results were obtained. The trajectories of the maximum principal stresses for the plate as well as the distribution contours of its fibre orientation angles and the fibre volume fraction are shown in Figure 3-5.
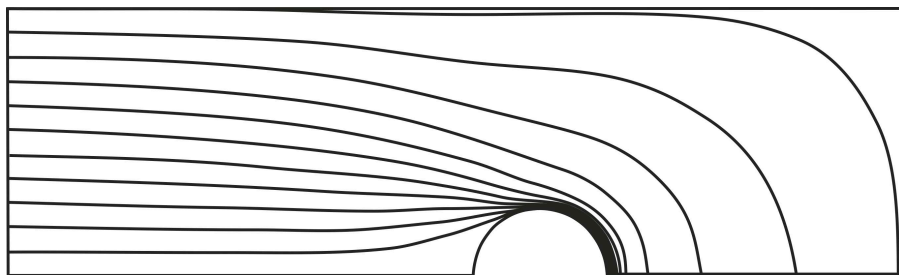

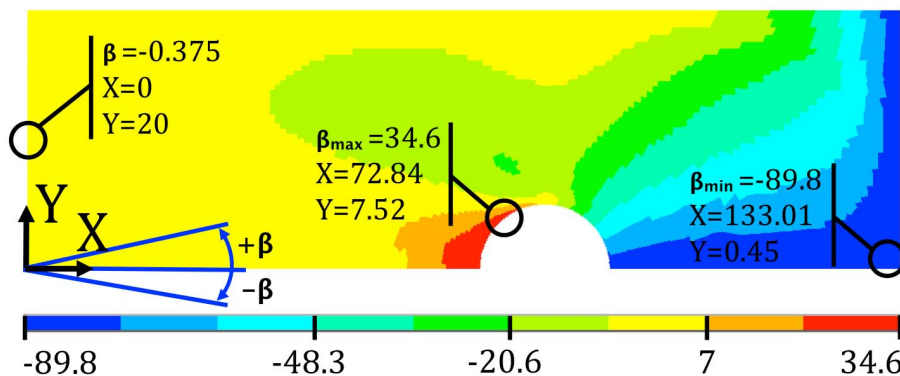**Figure 3.** The trajectories of the maximum principal stresses for the plate.

Figure 4. The distribution contour of the fibre orientation angles for the plate. The angles are measured in degrees.
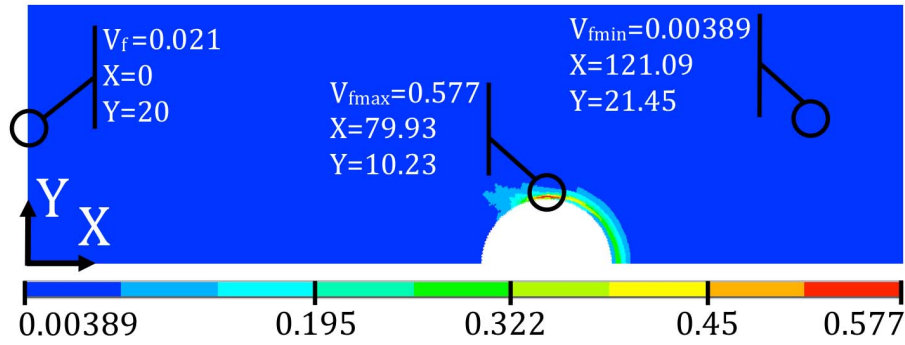
Figure 5. The distribution contour of the fibre volume fraction for the plate.

The contour of stress distribution along fibres (σ_1) is illustrated in Figure 6. As is seen in Figure 6, the value of the maximum stress concentration factor along fibres ($K_{tmax} = \sigma_{1max}/\sigma_o$) is 28.03 and its coordinate location practically coincides with the position of the maximum fibre volume fraction (V_{fmax}). It is interesting that the value of V_{fmax} increases by 27.48 times in comparison with the value of the fibre volume fraction (Figure 5), which has the coordinate location (0,20). In fact, the strength of the composite material depends on the fibre volume fraction. The ultimate tensile strength of the composite material in the fibre direction (σ_f^*) can be calculated by Equation (3) taken from [16]:

$$\sigma_f^* = \sigma_{fmax} \times V_f + (\sigma_m)_{\varepsilon 1max} \times (1 - V_f), \qquad (3)$$

where σ_{fmax} is maximum fibre tensile stress in the fibre direction, $(\sigma_m)_{\varepsilon 1max}$ is matrix stress at a matrix strain equal to the maximum tensile strain in the fibres.
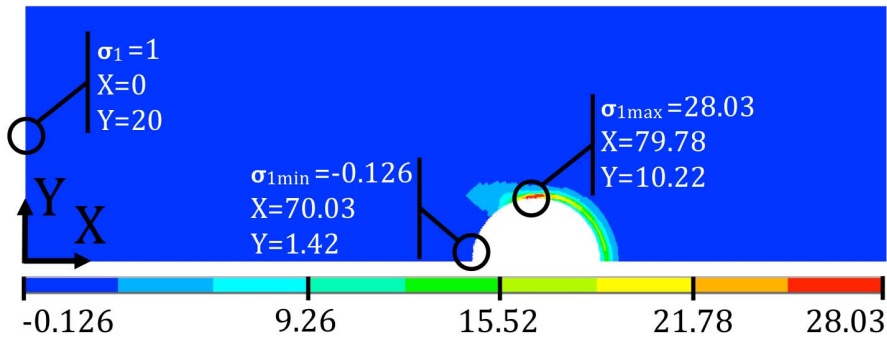

Figure 6. The contour of stress distribution along fibres. The stress is measured in Pa.

To estimate load-carrying capability a simplified failure criterion was used. The failure criterion is calculated by Equation (4). The composite material fails when $\zeta \geq 1$. It is known that $\sigma_f^* = 2724$ (MPa) at $V_f = 0.577$ [15]. $(\sigma_m)_{\varepsilon 1max}$ is not taken into account as $\sigma_{fmax} >> (\sigma_m)_{\varepsilon 1max}$. The ζ can be obtained for each element knowing σ_1, V_f and σ_{fmax}. The distribution contour of the failure criterion (ζ) is shown in Figure 7 when $\zeta_{max} = 1$. As is seen in Figure 7, the value of the maximum failure criterion (ζ_{max}) increases by 2 times in comparison with the value of the ζ located at the point (0,20), while in the structure with rectilinear reinforcement (orthotropic material) under identical conditions the value of the ζ_{max} increases by 16.4 times. It has been established that the shear stress for the curvilinear reinforcement structure is low and does not lead to matrix cracking but the compression stress transverse to fibres (σ_2) in zone B (Figure 2) is high and causes the local crumpling of the material in the zone.
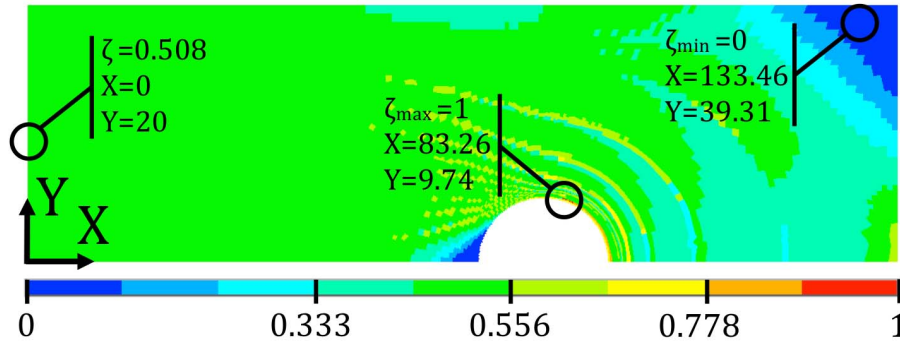
Figure 7. The distribution contour of the failure criterion (ζ).

$$\zeta = \sigma_1 / \sigma_f^*$$ (4)

The iterative process is completed when the values of $\sigma_{1max}/\sigma_{1o}$ and ζ_{max}/ζ_o are changed simultaneously not more than by 1% between iterations. Here σ_{1o} and ζ_o are the values of σ_1 and ζ located at the point (0,20). Seven iterations are necessary to fulfill the conditions. The functions $\sigma_{1max}/\sigma_{1o}$ (iterations) and ζ_{max}/ζ_o(iterations) are shown in Figure 8. The total elapsed time of the analysis is 42 hours.
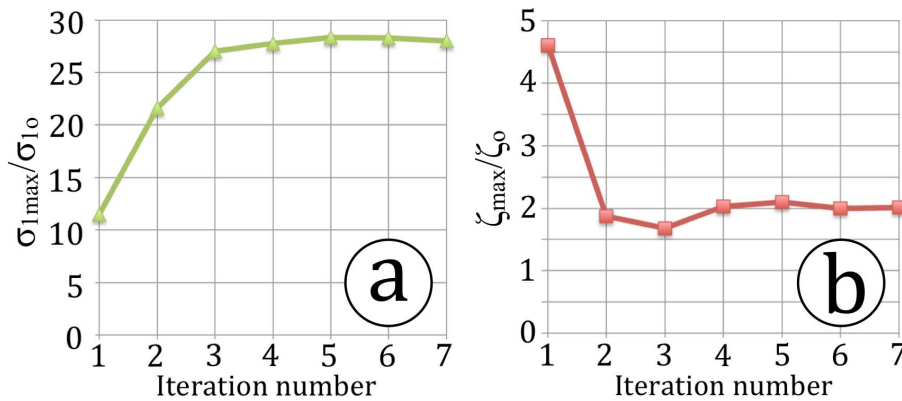

Figure 8. a – the function $\sigma_{1max}/\sigma_{1o}$ (iterations) at point (79.78,10.22); b – the function ζ_{max}/ζ_o (iterations) at point (83.26,9.74). See Figures 6,7.

5. Conclusions

It was demonstrated that the curvilinear reinforcement structure significantly increases the load-carrying capability. The simplified failure criterion was used to obtain the quantitative assessment of the load-carrying capability and understand effectiveness of the structure. It appears that the load-carrying capability for the curvilinear reinforcement structure increases by 8.2 times in comparison with the rectilinear reinforcement structure. However, it is necessary to fulfill more detailed investigation assessing the strength of the obtained structure according to specified criteria and taking into account the actual failure mechanisms of fibre composites. Applying the method of modelling, it is possible to design advanced joints between composite and metal components.

Acknowledgements

References

[1] M. Heller, R. Kaye, L.R.F. Rose. Gradientless finite element procedure for shape optimization. Journal of Strain Analysis for Engineering Design, vol. 34 (5):323-336, 1999.

[2] S.K. Dhir. Optimization of openings in plates under plane stress. AIAA Journal, vol. 21(10):1444–1447, 1983.

[3] P. Pedersen, L. Tobiesen, S.H. Jensen. Shapes of orthotropic plates for minimum energy concentration. Mechanics of Structures and Machines, vol. 20(4):499–514, 1992.

[4] A. Muc. Effectiveness of optimal design with respect to computational models for laminated composite structures weakened by holes. Structural optimization, vol. 16(1): 58–67, 1998.

[5] P. Pedersen. On optimal shapes in materials and structures. Structural and Multidisciplinary Optimization, vol. 19(3):169–182, 2000.

[6] H. Engels, W. Becker. Optimization of hole reinforcements by doublers. Structural and Multidisciplinary Optimization, vol. 20(1): 57–66, 2000.

[7] M.W. Hyer, R.F. Charette. Innovative design of composite structures: use of curvilinear fiber format to improve structural efficiency, University of Maryland Technical Report, University Park, Maryland, USA, pp. 87–5, 1987.

[8] C. Mattheck. Design in Nature: Learning from Trees. Springer-Verlag Berlin Heidelberg, Heidelberg, 1998.

[9] H. Cho, R. Rowlands. Optimizing Fiber Direction in Perforated Orthotropic Media to Reduce Stress Concentration. Journal of Composite Materials, vol. 43(10):1177-1198, 2009.

[10] J. Huang, R.T. Haftka. Optimization of fiber orientations near a hole for increased load-carrying capacity of composite laminates. Structural and Multidisciplinary Optimization, vol. 30(5):335-341, 2005.

[11] N. Banichuk, V. Saurin, A. Barsuk. Optimal orientation of orthotropic materials for plates designed against buckling. Structural optimization, vol. 10(3-4):191-196, 1995.

[12] M.W. Hyer, R.F. Charette. Use of curvilinear fiber format in composite structure design. AIAA Journal, vol. 29(6):1011-1015, 1991.

[13] M. Bauccio. ASM Metals Reference Book. ASM International, Materials Park, OH, 1993.

[14] A.V. Malakhov, A.N. Polilov. Construction of trajectories of the fibers which bypass a hole and their comparison with the structure of wood in the vicinity of a knot. Journal of Machinery Manufacture and Reliability, vol. 42(4):306-311, 2013.

[15] Hexcel HexPly 8552 Epoxy matrix product data sheet, 2012.

[16] R.M. Jones. Mechanics of Composite Materials. Taylor & Francis, Philadelphia, 1999.

[17] A.M. Jasso, J.E. Goodsell, A.J. Ritchey, R.B. Pipes, M. Koslowski. A parametric study of fiber volume fraction distribution on the failure initiation location in open hole off-axis tensile specimen. Composites Science and Technology, vol. 71(16):1819-1825, 2011.